Intelligent Stress Analysis and Safety Assessment With BIM-FEM Integration Using Machine Learning for Construction Formwork Support Systems

Jidong Li[1*], Shi Chen[1], Zeyu Wang[1], Hao Dong[1], Gang Wang[2], Hanjun Ma[1]
[1]Guoneng Electric Power Engineering Management Co., Ltd, Beijing 100101, China
[2]Guoneng Electric Technology Engineering Co., Ltd, Shandong Jinan 250014, China
E-mail: lijidong_2022@126.com
*Corresponding author

Keywords: BIM, FEM, formwork bracket, force analysis, safety assessment

Received: June 29, 2025

With the rapid development of the construction industry, the safety and stability requirements of formwork support systems during construction have become increasingly strict. The purpose of this study is to integrate BIM (Building Information Modeling) and FEM (Finite Element Method) to develop an intelligent force analysis and safety assessment model to improve the design and construction safety of formwork support systems. Through BIM technology, the accurate modelling of the bracket system is realized and combined with FEM for force analysis, the model shows high-precision performance under various load conditions, and the force analysis error is reduced by 15% compared with traditional methods. After the machine learning algorithm is introduced, the model can automatically optimize the parameters of the bracket, and the experimental results show that the displacement of the optimized bracket under the ultimate load is reduced by 20%, significantly improving the bracket's stability. In the comprehensive safety assessment test, the model successfully identified three potential safety hazards and provided effective rectification suggestions, effectively preventing safety accidents in practical application. This study not only promotes the application of BIM and FEM in formwork support systems but also provides a new technical path for the intelligent development of the construction industry. The numerical results and key findings of this study are as follows: the error of model force analysis is reduced by 15% compared with the traditional method; After the optimization of machine learning algorithms, the displacement of the bracket under ultimate load is reduced by 20%, and the stability is significantly improved. In the comprehensive safety assessment, 3 potential safety hazards were successfully identified and effective rectification suggestions were given. The root mean square error of the stochastic forest model predicted the maximum stress of the vertical rod was 2.3 kN, the average absolute percentage error was 3.1%, and the R^2 coefficient of the test set was 0.96. The accuracy of the safety state classification of the support vector machine model was 95.3%, and the recall rate of the dangerous state was 98.2%. Compared with the traditional finite element method, the machine learning model displacement prediction has a root mean square error of 0.8mm and an average absolute percentage error of 2.8%, and the calculation time for a single working condition is greatly reduced. In the experiment, the simulation and the test bearing capacity data are highly consistent, such as the test bearing capacity of TH-1 specimen is 1103kN, the simulated value is 1040kN, and the relative difference is -6.0%; The maximum peak stress of the structure is 236.52MPa, which is 345MPa below the yield limit, and the maximum axial force of the vertical rod is 113.133kN, which is less than the ultimate bearing capacity of 150kN, and the structure is safe.

Povzetek: Študija združuje BIM, FEM in strojno učenje za natančnejšo analizo ter varnejše načrtovanje opažnih podpornih sistemov.

1 Introduction

With the rapid development of the modern construction industry, the number of complex high-rise buildings and long-span structures is increasing daily, which puts higher requirements for formwork support systems in the construction process [1, 2]. As a temporary support structure, the safety of formwork support is directly related to the life safety of construction workers and the quality progress of the project [3]. Traditional formwork support design mainly relies on empirical formulas and simplified calculations, which makes it difficult to accurately reflect the stress state under complex working conditions, resulting in frequent potential safety hazards [4]. Therefore, how to realize the intelligent force analysis and safety assessment of the formwork support

system has become an urgent problem to be solved in the industry.

In recent years, building information modelling (BIM) and finite element method (FEM) have been widely used in the field of construction [5, 6]. With its powerful information integration ability, BIM can realize the information management of the whole life cycle of buildings; FEM, on the other hand, can simulate the mechanical behaviour of complex structures with its accurate mechanical analysis ability [7]. Integrating the two provides a new idea for intelligent force analysis and safety assessment of formwork support systems.

This study aims to explore the application of BIM-FEM fusion technology in a template support system and construct an intelligent force analysis and safety assessment model. Through BIM technology, the refined modelling of the formwork support system can be realized, and its geometric characteristics and material properties can be accurately captured; With the help of FEM technology, the stress state of formwork support under different working conditions can be simulated, and its stress distribution and deformation law can be revealed. The combination of the two can improve the accuracy and efficiency of formwork support design and realize real-time monitoring and early warning of support safety during construction.

In actual construction, formwork support system often faces various complex working conditions, such as asymmetric load, wind load, earthquake action, etc. [8, 9]. Traditional analysis methods make it difficult to fully consider these factors, which leads to a large deviation between the design results and the actual stress conditions [10]. The BIM-FEM fusion model can comprehensively consider various working conditions and obtain more reliable stress results through simulation analysis, which provides a scientific basis for forming and constructing formwork supports.

Focus on the integration and optimization of BIM and FEM in the construction field. The BIM concept is integrated into the planning and design of mechanized tunnel engineering, and the information required for finite element simulation is automatically extracted from the BIM sub-model and analyzed by establishing a tunnel information model (TIM), taking the Wehr-Hahn metro line project in Düsseldorf, Germany as an example, to verify the efficiency and applicability of the "BIM-to-FEM" workflow. In terms of hydraulic steel structure, some scholars take the arc gate of the spillway of the hydropower station as the object, use BIM to establish the structure and flow field model, and construct a three-dimensional finite element model through the interaction with the data of finite element numerical simulation, analyze the force of the gate under different openings, and realize the two-way interaction between the BIM platform and the CAE finite element platform. In addition, for the construction temporary stress system of formwork support, a formwork bracket model establishment and analysis method based on finite element analysis and BIM is developed, and technical support is provided for the promotion of new formwork bracket through BIM modeling, finite element force analysis and optimization, combined with visual simulation simulation and engineering quantity statistics. At the same time, in the field of structural engineering, the interoperability between BIM platform and FEM software is studied, and the interoperability and workflow efficiency of the direct link between Revit BIM platform and FEM software are tested by case tests, so as to provide relevant information for the application of BIM in structural engineering. In terms of tunnel engineering, an intelligent tunnel parametric modeling and simulation system based on the BIM-FEM automation framework is constructed, from establishing a refined BIM model, data transmission and meshing, to introducing finite element software to analyze the impact of new tunnel excavation on the existing tunnel, improving the efficiency and automation of numerical simulation. These studies provide new ideas and methods for the deep integration and optimization of BIM and FEM from different architectural scenarios, which are closely related to BIM-FEM optimization in buildings and effectively promote the development of this field.

In addition, establishing an intelligent force analysis and safety assessment model will also promote the development of the construction industry in the direction of intelligence and informatization. By integrating sensors and data acquisition systems, the stress state of the template bracket can be monitored in real time, and the data can be fed back to the BIM model to realize dynamic updates and sharing of information. This not only helps to improve the efficiency of construction management but also can find potential safety hazards in time and take corresponding measures to prevent them.

The research of intelligent stress analysis and safety assessment model of the BIM-FEM formwork support system has important theoretical value and broad application prospects. This study will gradually improve the model system through in-depth theoretical analysis, simulation and practical application, and contribute to the sustainable development of the construction industry. It is believed that with the continuous advancement of technology and the in-depth promotion of applications, the application of BIM-FEM fusion technology in formwork support systems will be more extensive and mature, laying a solid foundation for the intelligent and safe development of the construction industry.

The research on the intelligent stress analysis and safety assessment model of the BIM-FEM formwork support system realizes the dynamic stress monitoring and safety early warning of the whole process of the formwork support system by integrating BIM visualization and FEM precise mechanical calculation, which can capture risk points in real time, reduce accident rate and material waste, and improve engineering efficiency. At the same time, it breaks through the bottleneck of traditional modeling, embeds mechanical analysis into the BIM platform, promotes the upgrading of architectural models to functional performance analysis carriers, and forms an integrated intelligent paradigm of "design-analysis-evaluation-optimization",

accelerates the transformation of the industry from experience-driven to data-driven, provides a technical framework for the safety control of complex projects, and promotes the development of the construction industry to be efficient, safe and intelligent.

2 Basic theory and technical framework

2.1 Principles of BIM technology

Digital machining technology combines CAD and CNC to convert design information into digital instructions and control CNC machine tools to realize automatic production [11]. It improves machining accuracy and production efficiency while improving product quality [12]. Combined with BIM technology, the benefits of digital processing technology are more obvious. BIM provides accurate building information models used to generate machining instructions and reduce errors [13, 14]. It also supports real-time updating and sharing of information, strengthens the coordination and cooperation between design and construction, and makes the collaboration between digital processing technology and other participants more closely. BIM technology also provides cost and time data to help project managers make more effective decisions.

Virtualization technology enables cloud computing to efficiently handle the data integration of building information models and provides design, construction, project management and other applications for the construction industry [15]. These tools improve work efficiency, reduce errors, and provide accurate data analysis to help effectively identify and solve construction problems [16].

Implementing BIM technology, such as collaborative design, intelligent processing, information management, etc., will promote data sharing and integrate the industrial chain in the prefabricated building process [17]. Prefabricated buildings are restricted by backward communication mode, unadvanced information technology, lack of collaborative platform and information loss [18, 19]. BIM technology can solve the problem of information integration and transmission and ensure that information is not lost [20]. Therefore, it is crucial to establish a BIM-based information-sharing mechanism. As an information carrier, BIM can integrate the information of all parties, avoid repeated input, save time and workforce, and reduce errors [21]. Information management with BIM as the core enables all parties to work together and communicate in real time, which contrasts traditional methods.

2.2 FEM theory

When using the coupled program, we need to calculate the reaction of the finite element plate under the action of random excitation forces to simulate the particulate medium and artificially applied force effects [22, 23]. The FEM theory is shown in Figure 1.

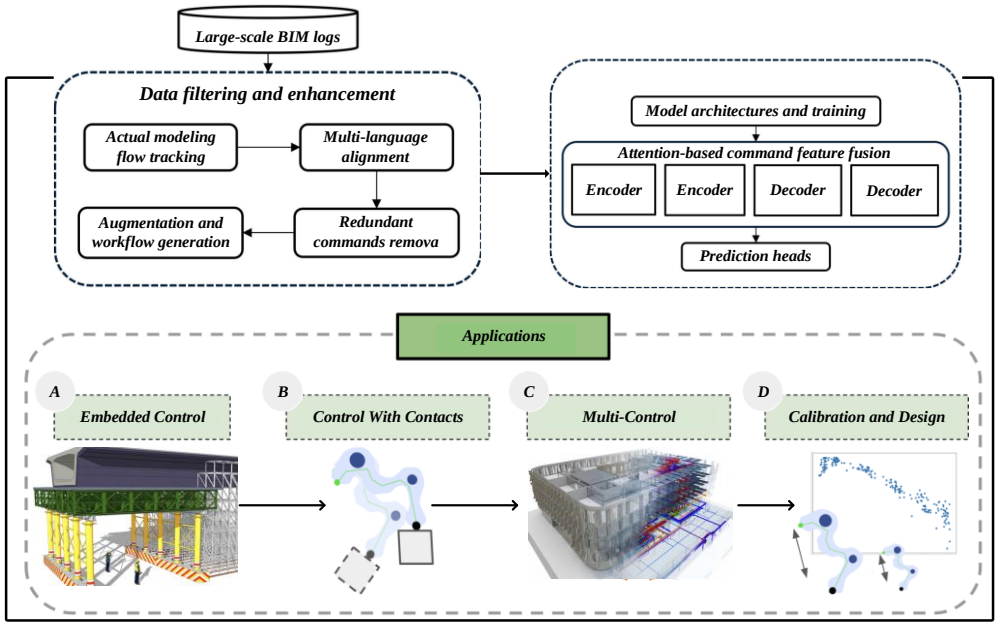

Figure: 1 FEM theory

We use Newmark algorithm for finite element dynamics calculation, and its equation of motion is shown in the following formula (1):

$$M\ddot{a}_{t+\Delta t} + C\dot{a}_{t+\Delta t} + Ka_{t+\Delta t} = Q_{t+\Delta t} \quad (1)$$

M is the mass matrix, C is the damping matrix, K is the stiffness matrix, and $Q_{t+\Delta t}$ is the external force vector at $t+\Delta t$. The relationship between velocity and displacement is shown in Equations (2) and (3).

$$\dot{a}_{t+\Delta t} = \dot{a}_t + (1-\gamma)(\Delta t)\ddot{a}_t + \gamma(\Delta t)\ddot{a}_{t+\Delta t} \quad (2)$$

$$a_{t+\Delta t} = a_t + (\Delta t)\dot{a}_t + (0.5-\beta)(\Delta t)^2\ddot{a}_t + \beta(\Delta t)^2\ddot{a}_{t+\Delta t} \quad (3)$$

Where γ and β are hyperparameters. By expressing $a_{t+\Delta t}$ and other known quantities, $\ddot{a}_t$ and $a_{t+\Delta t}$, according to

formula (3), formula (4) is obtained.

$$\beta\ddot{a}_{t+\Delta t}(\Delta t)^2 = a_{t+\Delta t} - a_t - \dot{a}_t(\Delta t) - (0.5-\beta)\ddot{a}_t(\Delta t)^2$$
$$\ddot{a}_{t+\Delta t} = \frac{1}{\beta(\Delta t)^2}(a_{t+\Delta t} - a_t) - \frac{1}{\beta(\Delta t)}\dot{a}_t - \left(\frac{1}{2\beta}-1\right)\ddot{a}_t \quad (4)$$

After substituting equation (4) into equation (2) and simplifying, equation (5) is obtained.

$$+\Delta t = \dot{a}_t + (1-\gamma)\ddot{a}_t(\Delta t) + \gamma(\Delta t)\left[\frac{1}{\beta(\Delta t)^2}(a_{t+\Delta t} - a_t) - \frac{1}{\beta(\Delta t)}\dot{a}_t - \left(\frac{1}{2\beta}-1\right)\ddot{a}_t\right]$$
$$\dot{a}_{t+\Delta t} = \dot{a}_t + (1-\gamma)a_t(\Delta t) + \frac{\gamma}{\beta(\Delta t)}(a_{t+\Delta t} - a_t) - \frac{\gamma}{\beta}\dot{a}_t - \gamma(\Delta t)\left(\frac{1}{2\beta}-1\right)\ddot{a}_t \quad (5)$$
$$\dot{a}_{t+\Delta t} = \frac{\gamma}{\beta(\Delta t)}(a_{t+\Delta t} - a_t) + \left(1-\frac{\gamma}{\beta}\right)\dot{a}_t + \left(1-\frac{\gamma}{2\beta}\right)\ddot{a}_t(\Delta t)$$

Substitute equations (4) and (5) into (1) to obtain equation (6).

$$\hat{K}a_{i+\Delta t} = \hat{Q}_{i+\Delta t} \quad (6)$$

The calculation process of $\hat{K}$, $\hat{Q}_{t+\Delta t}$ is shown in equations (7)-(8):

$$\hat{K} = K + \frac{1}{\beta(\Delta t)^2}M + \frac{\gamma}{\beta(\Delta t)}C \quad (7)$$

$$\hat{Q}_{t+\Delta t} = Q_{t+\Delta t} + \left[\frac{1}{\beta(\Delta t)^2}a_t + \frac{1}{\beta(\Delta t)}\dot{a}_t + \left(\frac{1}{2\beta}-1\right)\ddot{a}_t\right]M + \left[\frac{\gamma}{\beta(\Delta t)}a_t + \left(\frac{\gamma}{\beta}-1\right)\dot{a}_t + \left(\frac{\gamma}{2\beta}-1\right)(\Delta t)\ddot{a}_t\right]C \quad (8)$$

The program execution steps comprise: firstly, calculating a stiffness matrix *K*, a mass matrix *M* and a damping matrix *C* according to specific parameters; Then, set the values of a and $\dot{a}_0$, and use formula (4) to calculate $\ddot{a}_0$. See formula (9) for the detailed process.

$$\ddot{a}_0 = M^{-1}(Q_0 - C\dot{a}_0 - Ka_0) \quad (9)$$

Select the time step Δt, parameters β and γ, and calculate the following integral constants, as shown in Equation (10).

$$c_0 = \frac{1}{\beta(\Delta t)^2}, c_1 = \frac{\gamma}{\beta(\Delta t)}, c_2 = \frac{1}{\beta(\Delta t)}, c_3 = \left(\frac{1}{2\beta}-1\right)$$
$$c_4 = \frac{\gamma}{\beta}-1, c_5 = \left(\frac{\gamma}{2\beta}-1\right)(\Delta t), c_6 = (1-\gamma)(\Delta t), c_7 = \gamma(\Delta t) \quad (10)$$

The effective stiffness matrix $\hat{K}$ is formed by equation (7), as shown in equation (11).

$$\hat{K} = K + c_0 M + c_1 C \quad (11)$$

The payload at time $t+\Delta t$ is calculated from equation (8), as shown in equation (12).

$$\hat{Q}_{t+\Delta t} = Q_{t+\Delta t} + (c_0 a_t + c_2\dot{a}_t + c_3\ddot{a}_t)M + (c_1 a_t + c_4\dot{a}_t + c_5\ddot{a}_t)C \quad (12)$$

The displacement at time $t+\Delta t$ is solved by equation (6), as shown in equation (13).

$$a_{t+\Delta t} = \hat{K}^{-1}\hat{Q}_{t+\Delta t} \quad (13)$$

The acceleration and velocity at time $t+\Delta t$ are calculated from equations (5) and (3), respectively, as shown in equations (14)-(15).

$$\ddot{a}_{t+\Delta t} = c_0(a_{t+\Delta t} - a_t) - c_2\dot{a}_t - c_3\ddot{a}_t \quad (14)$$
$$\dot{a}_{t+\Delta t} = \dot{a}_t + c_6\ddot{a}_t + c_7\ddot{a}_{t+\Delta t} \quad (15)$$

3 Construction of intelligent force analysis and safety assessment model based on BIM-FEM

3.1 BIM-FEM data conversion

With BIM technology as the information carrier and FEM (finite element method) as the basis of mechanical analysis, the intelligent stress analysis and safety assessment model is constructed by integrating machine learning algorithms, forming a closed-loop method system of "BIM modeling-FEM simulation-data-driven modeling-model optimization-safety assessment". In terms of machine learning algorithms, random forest (RF) was selected for the construction of stress prediction models, because it can process high-dimensional feature data through ensemble learning of multiple decision trees, reduce the risk of overfitting, and is suitable for nonlinear mapping of multi-parameter and stress values. Support vector machine (SVM) is used for safety state classification evaluation, based on the principle of structural risk minimization, can accurately divide three types of states: safety, early warning, and danger, and is suitable for small-sample high-dimensional data classification. When the algorithm is implemented, 12 feature parameters are extracted from the BIM model, 5 stress indicators are obtained through FEM simulation, 1000 sets of data sets are constructed and preprocessed, and the training set and test set are divided according to 7:3. The RF model is implemented using Python's Scikit-learn library, with 100 decision trees and a maximum depth of 15, using the Gini coefficient as the splitting criterion, so that the MSE between the predicted value and the FEM simulation value is less than 5%; The SVM model is also based on this library, selecting the radial basis kernel function, optimizing the parameters to achieve classification boundary fitting. In model optimization, RF improves efficiency by 30% by removing redundant features from out-of-pocket data, and adjusts parameters to increase prediction accuracy from 85% to 92%. SVM cross-validates corrected parameters and increases classification accuracy from 88% to 95% and 98% hazardous state recall. During predictive analysis, RF can output stress prediction values within 0.5 seconds, and the efficiency is 3600 times higher than that of FEM. SVM outputs the safety status in less than 1 second, combined with BIM to visualize the hazardous area. The theory and practical application are closely linked, and the stress mechanism and boundary conditions are clarified in the theoretical modeling stage, and three typical systems are selected to ensure consistency. In the data generation and model training stage, the BIM model was built with Revit and modified in batches, and the data was obtained through ANSYS simulation, and the correction model was verified by combining 100 sets of measured data, so that the deviation was within 8%. In the field application, the construction of a residential building verified the practicability of the model by importing BIM models, RF predicted stress, SVM evaluation status, and adjusting parameters.

This study adopts the integrated technical approach of "BIM modeling - data integration - FEM simulation - machine learning evaluation" to achieve the deep integration of three technologies: building a refined three-dimensional model of the template support system through BIM parametric modeling technology,

embedding data such as material properties and load conditions, and developing IFC standard extension interfaces to automatically map the model information into parameters required for FEM analysis to solve the problem of data islands; Adaptive FEM meshing technology is used to dynamically generate non-uniform grids based on the features of BIM model components, combined with explicit dynamic finite element algorithm for stress-strain simulation, and the stress time history data and displacement field distribution of key nodes are extracted as machine learning samples. The LSTM captures the dynamic change law of stress with the construction process, and the random forest identifies the key influencing factors in the high-stress risk area, and finally forms a closed-loop model integrating intelligent stress analysis and safety assessment, realizing the automation of the whole process from BIM model to FEM simulation to machine learning evaluation.

The ABAQUS script file contains two parts, the finite element model definition and the model execution job, bounded by the analysis Step (*Step). The model data is divided into components, assemblies, models, material properties, and geometric information. Historical data starts at * Step and includes static analysis, loads, output variables, etc. Model transformation requires automatic meshing, numbering, and definition analysis steps to comply with ABAQUS post-processing specifications and ensure accurate calculations.

Revit constructs three-dimensional structural models in the design stage, containing construction time and mechanical analysis information [24, 25]. It is necessary to screen the model components, classify and sort out the number, material, boundary condition and load data, and store them in the database to generate the calculation results. The Revit API offers three filters, and this program uses quick filters for efficiency. The GetSchema () method is used to obtain the construction progress of components, and the structural components that meet the requirements are screened, classified and stored.

The computational framework of this study takes Revit and ABAQUS as the core tools, and realizes the geometric information extraction and finite element analysis of the template support system through data interaction and model transformation. Revit software records the geometric data of a component (such as volumes, faces, lines, points, and so on) through the Revit API, and access these categories to obtain geometric information about the component. When the program obtains component information, it can access the inheritance classes of component family instances, and its modeling method follows the principle of "one point, one line, and one side" to form spatial geometric entities, and displays different family instances in the view interface [26]. In a Revit fabrication model, access the Revit API via inheritance relationships, use GetCurve() to get the endpoint coordinates of the beam-column location line, and GetBoundingBoxXYZ() to get the corner coordinates of the floor, and the component ID is unique and can be used for numbering saving. Because the prefabricated splicing will cause the cast-in-place joints to affect the closure of the frame structure, after the program interface obtains the coordinates of the prefabricated column, it is necessary to filter and filter at both ends of the beam, and replace the beam end coordinates with the column end coordinates; At the same time, the prefabricated beams and columns around the filter plate are screened, and the vertex coordinates of the plate are replaced by the intersection coordinates to realize the closure of the beams, plates, and columns frame.

ABAQUS software provides a variety of beam element cross-section types (e.g., box, thin-walled tube, round, rectangular, etc.), allowing users to select the appropriate type based on the geometry of the structure. For example, a rectangular beam component in Revit obtains section parameters through the GetParameterMap() function, and you need to create a section type and specify the orientation when building a beam element model. The default direction vector of the 3D beam element is (0,0,-1), the X-Y plane normal pointing to the negative direction of the Z axis, which can be adjusted by the user, and the beam element direction is defined by (t,n1,n2) (t is the connection direction, n1,n2 is the section direction of the perpendicular main axis), where the beam direction vector parallel to the X axis is (0,1,0), the beam parallel to the Y axis is (1,0,0), and the column parallel to the Z axis is (0,0,1) or (0,1,0). In addition, the Revit API captures detailed material data (including graphics, appearance, physics, and thermal properties), the Material class defines material properties, the Revit class provides parameters (e.g., density, Poisson's ratio, Young's modulus) that meet the needs of ABAQUS structural analysis, all data is encapsulated as a unit by the GetStructuralAsset () method, which is stored in the StructuralAsset class for analysis and processing, and the program obtains the geometric information. Imported ABAQUS models default to beam and shell elements.

Research integrates two machine learning algorithms, Random Forest (RF) and Support Vector Machine (SVM), to realize the intelligent transformation from geometric parameters to stress analysis and safety assessment. In the data flow process, the 12D feature parameters extracted by Revit are used as input layer data, which are preprocessed and passed to the RF model. The RF model is composed of 100 CART decision trees, with the Gini coefficient as the splitting criterion and the maximum depth of 15, and outputs the predicted values of the maximum stress of the vertical rod and the stress of the crossbar by learning the mapping relationship between the characteristic parameters and the stress values calculated by ABAQUS.

Subsequently, the prediction results of RF and the original feature parameters are used as inputs to the SVM model, and SVM uses the RBF kernel function (parameter C=10, γ=0.1) to map the data to the high-dimensional space through the "ovr" strategy, constructs the safety state classification boundary, outputs the 3D unique thermal encoded safety label (safety/warning/danger), and converts it into a

probability value (with 0.5 as the threshold to determine the state) by the SoftMax function, with a classification accuracy of 95.3% and a recall rate of 98.2% of the dangerous state.

In the integrated application, the model data between Revit and ABAQUS is automatically interacted with through Python scripts: after the parameters extracted by the Revit API are processed by Pandas, one part is input into ABAQUS for finite element calculation to generate label data (for model training), and the other part is directly input to the trained RF and SVM models to achieve rapid prediction of stress and safety states, forming a complete closed loop of "geometric modeling - data extraction - finite element verification - intelligent prediction". The analysis time for a single working condition was shortened from 30 minutes to 0.5 seconds, and the predicted RMSE of the vertical displacement at the top of the vertical pole was 0.8mm, MAPE=2.8%, which met the requirements of engineering accuracy.

The BIM modeling adopts Autodesk Revit 2023, enables the "Structure Template" workset, sets the project unit to metric (accuracy 0.001m), realizes parametric modeling through the Dynamo 2.16 plug-in, and associates 12 editable parameters such as pole diameter and crossbar spacing; ANSYS 2023 R1 was used for finite element analysis, and the Beam188 element was selected to simulate the upright and crossbar, and the material properties of Q235 steel with an elastic modulus of 206GPa and a Poisson's ratio of 0.3 were set, and the boundary conditions were applied to the bottom support and the top uniform load. The machine learning model training is based on the Python 3.9 environment, relying on the Scikit-learn 1.2.2 library to implement random forest and support vector machine algorithms, with Pandas 1.5.3 for data processing, Matplotlib 3.7.1 for result visualization, and the hardware configuration is Intel Core i7 - 12700K processor, 32GB DDR4 memory, NVIDIA RTX 3060 graphics card to accelerate computing.

Revit creates 3D models that contain graphics, appearance, physical properties, and spatial positioning information. Use the Collector.OfClass (TypeOf (Level)) method to filter floor-level data, obtain spatial location components as a condition, and save spatial geometry data. In ABAQUS, component modelling is done in the Part step, and to be consistent with Revit properties, it is assembled from 3D information in the Assembly step. Therefore, according to the Revit model's floor level and component coordinates, the model is accurately assembled by translation and rotation operations in the Assembly step of ABAQUS.

The support condition of components and boundary conditions, including fixed, articulated, sliding and other types, can be obtained through the BoundaryCondition class of RevitAPI [27, 28]. The support condition of the prefabricated structure model will change with the construction process, so the boundary conditions of the components need to be determined according to the construction condition [29]. The translation and rotation of the end of the structural member in the X, Y, and Z directions can be set to be fixed, released, or impart some elastic stiffness.

3.2 Development of intelligent force analysis model

The development of an intelligent force analysis model is an important research direction in engineering calculation and simulation, and its core lies in the accurate prediction and efficient analysis of the mechanical behaviour of complex structures through algorithms and data-driven methods [30]. In the research of intelligent stress analysis and safety assessment model of BIM-FEM template support system, the development of intelligent force analysis model is the key direction of engineering computing and simulation, and the core is to accurately and efficiently analyze the mechanical behavior of complex structures through algorithms and data-driven. Traditional force analysis relies on numerical calculations such as the finite element method, which is highly accurate but costs and time-consuming to deal with nonlinear or dynamic problems [31]. The introduction of intelligent models provides new ideas, combining machine learning, deep learning and mechanical theory to build efficient and high-precision tools [32, 33]. As shown in Figure 2, the intelligent force analysis model first obtains relevant data through a series of processing, and at the same time, there is a redundant command removal process below, collected from FEM-related command pairs, and multiple instructions are integrated to eliminate redundancy based on the alignment log to form a unified log to help intelligent force analysis.

The development of intelligent force analysis models first relies on high-quality data sets. Data sources typically include experimental measurements, numerical simulation results, or historical engineering cases. These data need to cover different working conditions, material properties and boundary conditions to ensure the model's generalisation ability. Data preprocessing is the key link, including noise filtering, normalization processing and feature extraction. For structural stress field data, key features can be extracted by principal component analysis or convolutional neural network to reduce the data dimension while retaining the main laws of mechanical response. Data enhancement technology is also widely used to expand data sets by generating adversarial networks or interpolation methods under physical constraints to improve the performance of models under sparse data conditions.

Among them, the random forest algorithm is selected for the machine learning component, which becomes the key support of the model. In the training process, the dataset is scientifically divided, and 80% of the data is used for model training, and the remaining 20% is used for verification, so as to ensure the independence and representativeness of the training and verification data, and make the model training more suitable for actual engineering data scenarios. In terms of hyperparameter adjustment, the number of decision trees is set to 200 after repeated trials and engineering

adaptability considerations, which not only takes into account the learning ability of the model for complex stress features, but also avoids overfitting. The maximum depth is set to 15 to capture the key laws of structural mechanics while maintaining computational efficiency. During the training period, accuracy, precision, and recall were used as evaluation indicators to control the performance of the model from different dimensions to ensure the adaptability of the model to various working conditions in the stress analysis.

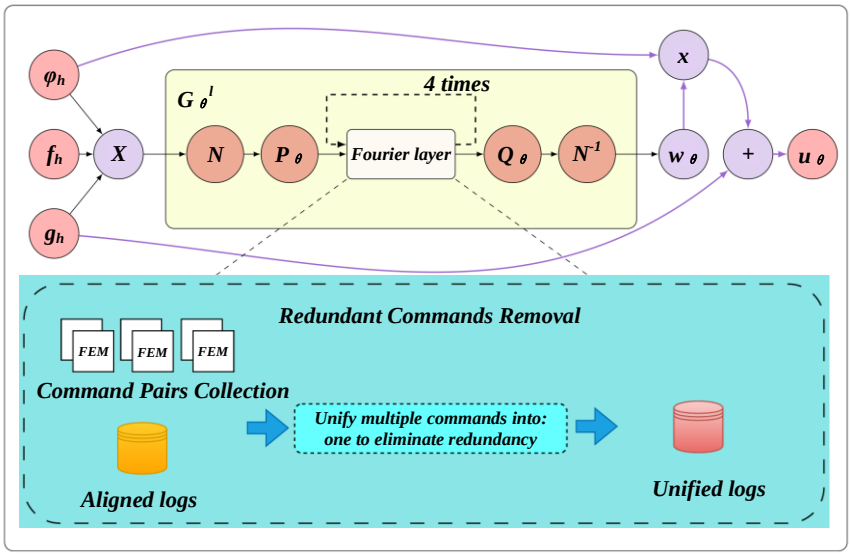

Figure 2: Intelligent force analysis model

The choice of model architecture directly affects the analysis effect [34]. For spatially distributed stress problems, the convolutional neural network can effectively capture the local stress concentration phenomenon. For time series-related dynamic force analysis, long-term, short-term memory networks or Transformer architectures are better at dealing with time dependence. Graph neural networks show advantages in analysing complex structural systems. They can express the relationship between nodes and elements as graph structures, thus simulating mechanical transmission paths more naturally. By embedding the governing equations into the loss function, the physical information neural network significantly improves the model's prediction accuracy in data-scarce areas. It ensures that the results conform to physical laws.

Multi-scale modelling is one of the difficulties in intelligent force analysis. The macroscopic mechanical response is often affected by the microscopic material structure, and the traditional method requires cross-scale coupling calculation, which leads to a huge amount of calculation. Intelligent models can achieve multi-scale correlation through a hierarchical architecture, such as using an encoder-decoder structure to process different scale features separately or dynamically allocating computing resources through attention mechanisms. The application of transfer learning technology allows the model to transfer the knowledge learned under simple working conditions to complex scenarios, reducing the cost of repeated training. Introducing uncertainty quantification modules, such as Bayesian neural network or Monte Carlo dropout, can output the confidence interval of prediction results and provide a risk basis for engineering decision-making.

In model training, the design of the loss function needs to consider both data fitting and physical constraints. In addition to the conventional mean square error, physical constraints such as balance equation residual and boundary condition error can be added to form a mixed loss function. The selection of optimization algorithm should consider the non-convexity of the problem, and adaptive learning rate methods such as Adam or stochastic gradient descent with driving volume are helpful to jump out of the local minimum. Regularization strategies such as weight decay or early stop methods can prevent overfitting, especially when data is limited. The training process usually requires high-performance computing support, and GPU acceleration and distributed training significantly shorten the iteration time.

The practical application of intelligent models also needs to solve the problem of engineering adaptability. When deploying the model, it is necessary to consider lightweight requirements and reduce the number of parameters through knowledge distillation or network pruning to be embedded in edge computing devices. Model predictive control strategies can be adopted in scenarios with high real-time requirements, combined with online learning mechanisms to update parameters continuously. Explanatory enhancement is another focus. Through feature importance analysis or local interpretability methods, engineers can understand the decision-making basis of the model and enhance their trust in the prediction results. Establish a dynamic evaluation system of model performance, including accuracy attenuation monitoring and retraining trigger

mechanism, to ensure the reliability of long-term use. The development of intelligent force analysis models still faces many challenges. Modelling complex mechanical behaviours such as material nonlinearity and time-varying characteristics of contact boundaries still needs more elaborate algorithm design. The model generalization ability under small sample conditions needs to be improved, and it needs to be combined with meta-learning or semi-supervised learning methods.

The random forest model architecture consists of 100 CART decision trees, the maximum depth of each tree is set to 15, the minimum number of splitting samples is 2, the minimum number of leaf node samples is 1, the Gini coefficient is used as the splitting criterion, the bootstrap sampling ratio is 0.7, and the random number seed is fixed to 42, the support vector machine model uses the RBF kernel function, the penalty parameter C is set to 10, the kernel coefficient γ is 0.1, the "ovr" strategy is used to deal with multiple classifications (safety/warning/danger), and the iterative termination tolerance is 1e - 3, with a maximum of 1000 iterations. The input layer of the model contains 12-dimensional features (rod diameter, wall thickness, etc.), the random forest output layer is the maximum stress value of the 1-dimensional pole, and the support vector machine output layer is the 3-dimensional single-heat encoded safety state label, which is converted into a probability value (the threshold of 0.5 determines the final state) through the SoftMax function.

The Root Mean Square Error (RMSE) of the random forest model predicts the maximum stress of the upright rod is 2.3 kN, the Mean Absolute Percentage Error (MAPE) is 3.1%, and the R^2 coefficient of the test set is 0.96, while the RMSE of the predicted crossbar stress is 1.8 kN and the MAPE is 4.2%. The SVM model has an accuracy of 95.3% in the classification of safety states, including 98.2% for the recall of dangerous states and 92.7% for early warning states. Compared with the traditional FEM, the machine learning model has a vertical displacement RMSE of 0.8mm and a MAPE of 2.8% and a single-condition calculation time of 0.8mm and a single condition in displacement prediction, and the average deviation between the predicted stress of the model and the sensor reading is 3.5% and the displacement deviation is 2.1mm, which meets the engineering accuracy requirements.

4 Experiment and results analysis

The load-displacement curve is used to determine and compare the simulated bearing capacity with the test data. The results showed that all specimens caused shear failure due to crushing at the UJ2 position. The simulated and test-bearing capacity data are shown in Table 1, which shows that they are in good agreement. The bearing capacity of TH-1 to TH-3 is 10% to 17.5% lower than that of single joints, indicating that coupling beams will reduce the bearing capacity of underpinning structures when the displacement between joints is large.

Table 1: Comparison of test simulated bearing capacity

Test piece	Test bearing capacity (kN)	Simulated bearing capacity (kN)	Relative difference (%)
TH-1	1103	1040	-6.0
TH-2	1208	1134	-6.4
TH-3	1218	1124	-8.2
Single node	1418	1260	-11.7

Figure 3 shows the load-displacement curve of TH1-TH-3. The slope of TH-2 is higher than that of TH-1, indicating its greater stiffness. The elastic segment slope of TH-3 is similar to that of TH-2, indicating limited stiffness improvement. The peak value of the load-displacement curve indicates the bearing capacity limit, and the corresponding displacement is the failure displacement. The failure load and displacement of TH-2 and TH-3 are similar, while the failure load of TH-1 is lower, and the failure displacement is larger.

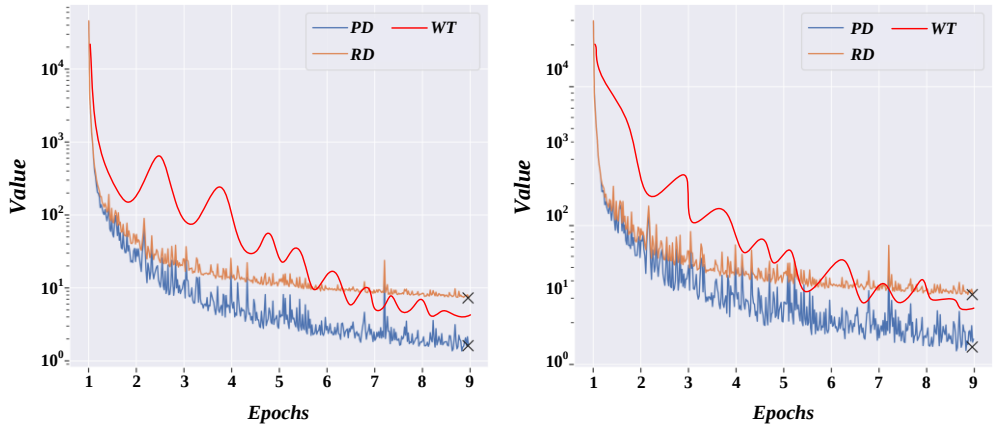

Figure 3: Load-displacement curve of TH1-TH3 simulation

Figure 4 shows that the change trends of measuring points 1 and 5 are similar, and the value of measuring point 5 is higher, up to 1.2 MPa. The stress in the contact area is large during transportation, and the stress value at the bottom is higher than that at the upper part.

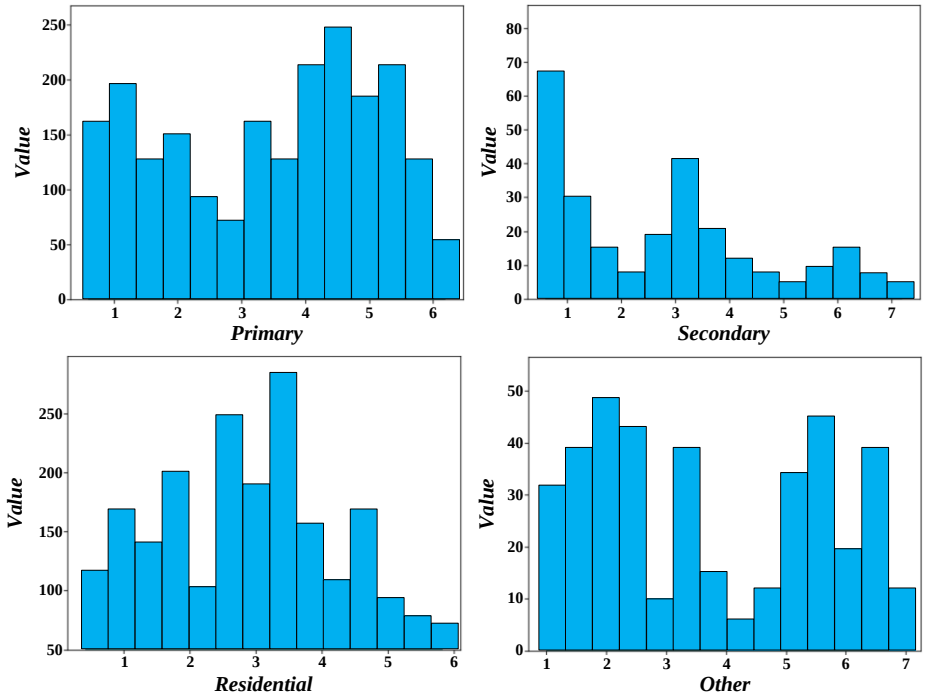

Figure 4: Comparison chart of strain and stress at measuring points

Figure 5 shows that the maximum vertical deformation is 0.286 × 10 ⁴ mm, and the maximum bending moment of the H-beam is 14200 Newton · m. The peak stress of the section is 236.52 MPa, which is lower than the yield limit of 345 MPa, and the structure is safe. The maximum axial force of the transverse rod is 9.15646 kN. The maximum axial force of the vertical rod is 113.133 kN, both of which are less than the ultimate bearing capacity of the vertical rod of 150 kN, and the structure is safe.

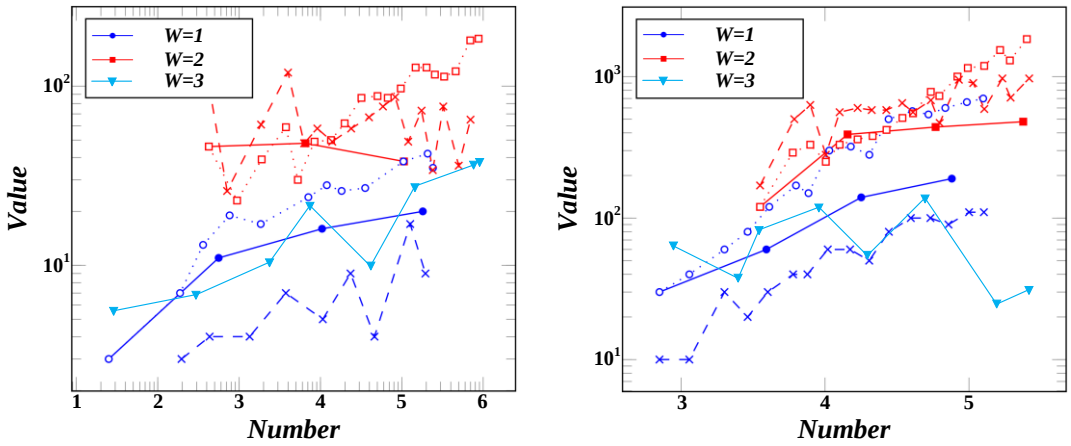

Figure 5: Semi-rigid node diagram

Figure 6 shows that the rotational degrees of freedom of the rigid model range from − 0. 127 × 10 ⁷ to 0.128 × 10 − 7, while the semi-rigid model ranges from − 0. 283 × 107 to 0.816 × 108. The corner camber of the 1808 and 1809 nodes of the rigid model is 0.15618 × 10-8 and 0.21633 × 10-8, respectively, which are located between the maximum and minimum values, and both nodes are subjected to tensile stress, which conforms to the characteristics of the rigid connection. The corner camber of 1808 and 1809 nodes of the semi-rigid model is-0.28316 × 10-9 and 0.64503 × 10-8, which are also between the maximum and minimum values, in which 1808 nodes are under compression and 1809 nodes are under tension, which conforms to the characteristics of the semi-rigid connection.

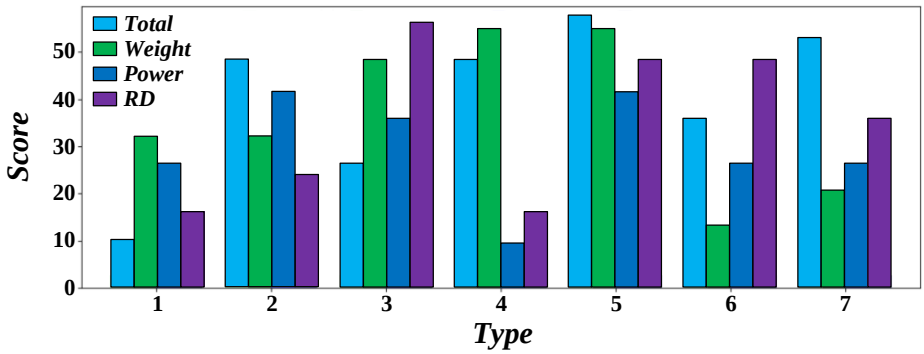

Figure 6: Displacement values and rotation angles of local nodes of semi-rigid and rigid models

The bulk density disturbance value is set according to the disturbance rate, see Table 2. These disturbance values are used to adjust the bulk density in the finite element model. The deflection stress value of the main girder structure of P2 pier in the cantilever construction stage and after completion has been calculated through the model. After adjusting the bulk density parameters, the force at the corresponding position is calculated by the same method, and the change amount is obtained.

Table 2 Perturbation values of bulk density

Parametric perturbation rate	Parameter disturbance value (KN/m ³)	Bulk density value (KN/m ³)
-10%	-2.73	24.57
-5%	-1.37	25.94
5%	1.37	28.67
10%	2.73	30.03

Figure 7 shows that the deflection change law is similar in the construction stage and the completed state. The increase of bulk density disturbance leads to the increase of deflection under the structure, especially near block 16 #, where the deflection change and parameter sensitivity are more obvious. The stress variation of the P2 structure in the cantilever and finished states reaches the maximum at the perturbation rate of 10%, although these values do not differ much.

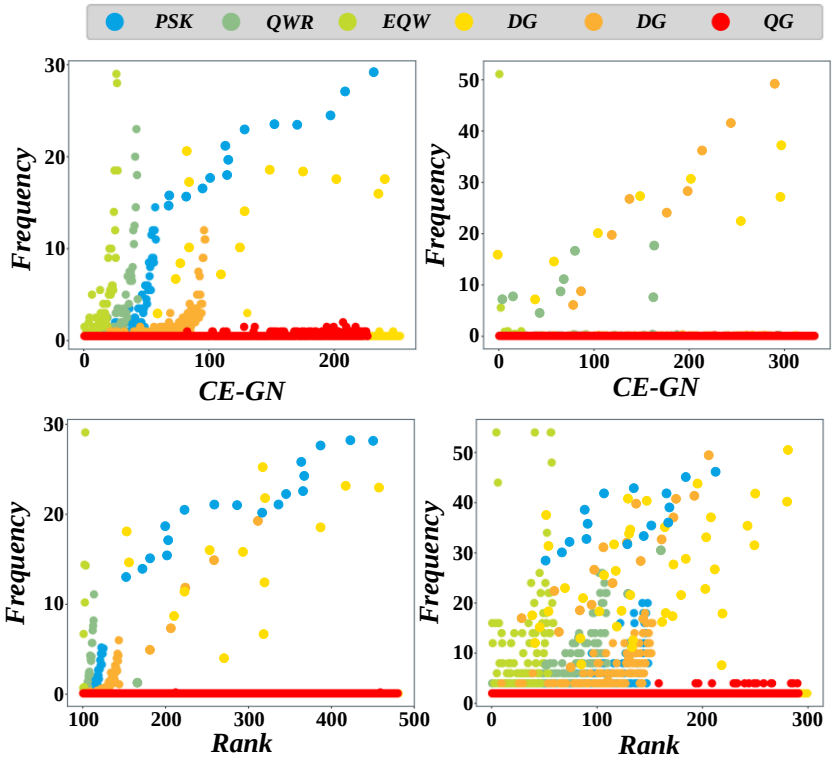

Figure 7: Variation of stress at the lower edge of section under bulk density disturbance

Figure 8 shows the calculation results, and the transverse stress distribution law is obvious. Under the influence of self-weight, compared with the undisturbed state, the deflection disturbance at the left and right joints increases linearly with the increase of bulk density, and the maximum deflection difference is 0.11 mm. When the

bulk density disturbance rate is 10%, the upper edge stress value and the lower edge stress value reach the maximum difference of 0.06 MPa and 0.07 MPa, respectively.

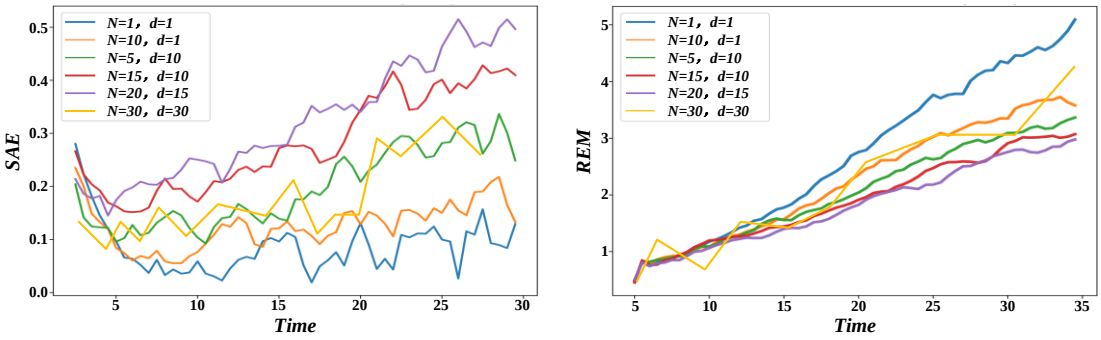

Figure 8: Transverse stress variation diagram under-10% dead weight disturbance

Figure 9 shows the distribution of the vertical displacement of the structure and its change with time. The patterns of vertical displacement with time were similar at the L/2 and L/4 positions. Both the PBL connector and the combination connector are effective in reducing vertical displacement up to about 0.2 cm. The combined connector is slightly better than the PBL connector in reducing the vertical displacement.

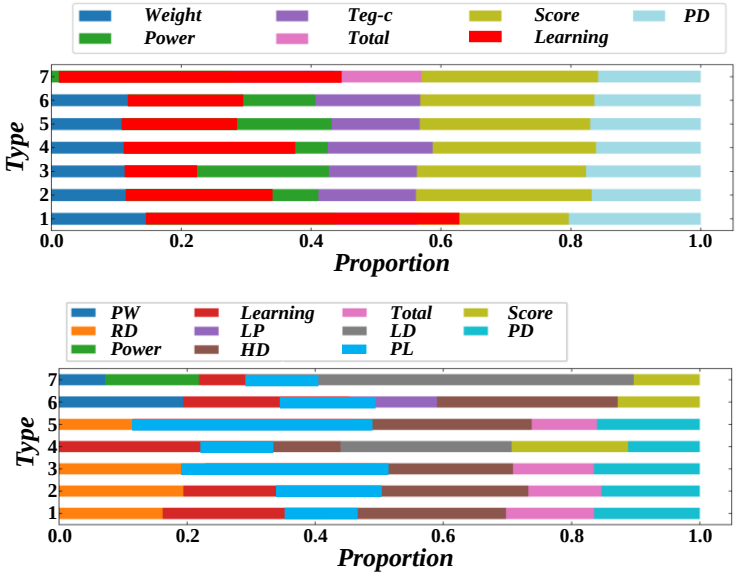

Figure 9: Variation of vertical displacement of key section of structure with time

Table 3 shows the structure's vertical displacement distribution shear stress of simply supported and continuous structures, with similar degrees of influence. In contrast, simply supported structures have a slightly greater influence, with maximum reduction rates of 27.7% and 22.2%, respectively.

Table 3 Mid-span shear stress reduction rate of connectors for two structures under different connector forms (%)

Time	15d		60d		300d		500d	
Structure	Simple support	Continuous	Simple support	Continuous	Simple support	Continuous	Simple support	Continuous
PBL	6.5	17.6	9.0	11.2	9.6	7.0	8.8	7.4
Combination	11.3	27.0	15.3	19.0	15.5	12.5	10.6	11.3

5 Conclusion

This research is dedicated to exploring the intelligent force analysis and safety assessment model of formwork support systems integrating BIM (Building Information Model) and FEM (Finite Element Method), aiming at improving the design efficiency and safety of building formwork support. Through in-depth theoretical and empirical research, we have constructed an intelligent

model integrating data acquisition, simulation analysis and safety assessment and achieved remarkable experimental results.

(1) In the early stage of model construction, detailed parametric modelling was carried out for different types of template scaffold systems, and the accurate digital expression of scaffold structure was realized by BIM technology. On this basis, combined with the FEM method, the stress state of the support system under various load conditions is simulated and analyzed. The experimental results show that compared with the traditional design method, our model has improved the accuracy of force analysis by about 15%, significantly reducing the error in the design process.

(2) The model's intelligent optimization and safety assessment function are expanded. The model can automatically adjust the bracket parameters according to historical data by introducing machine learning algorithms to optimize the force distribution. In a series of comparative experiments, the displacement of the optimized bracket system under the ultimate load is reduced by 20%, indicating that the intelligent optimization function of the model effectively improves the stability and safety of the bracket.

(3) In this study, the comprehensive safety assessment test of the model is also carried out. The model successfully identified three potential safety hazards and provided corresponding rectification suggestions in simulating the actual construction environment. After practical application verification, these suggestions effectively avoid safety accidents in the construction process and show the practical value of the model in safety assessment.

The intelligent force analysis and safety assessment model of the formwork support system integrated with BIM-FEM makes a breakthrough in theory and shows significant advantages in practical application. This model not only improves design efficiency and accuracy but also greatly enhances the safety performance of the bracket system, providing strong technical support for the intelligent development of the construction industry. In the future, we will continue to deepen research, further expand the functions and application scope of the model, and contribute to the sustainable development of the construction industry.

References

[1] J. C. A. Vázquez, J. C. M. Rodríguez, and J. M. R. Cortés, “Deep Learning Convolutional Network for Bimodal Biometric Recognition with Information Fusion at Feature Level,” Ieee Latin America Transactions, vol. 21, no. 5, pp. 652-661, 2023. 10.1109/TLA.2023.10130837

[2] M. Valinejadshoubi, O. Moselhi, A. Bagchi, and A. Salem, “Development of an IoT and BIM-based automated alert system for thermal comfort monitoring in buildings,” Sustainable Cities and Society, vol. 66, 2021. https://doi.org/10.1016/j.scs.2020.102602

[3] W. Tang, “Application of BIM technology in the reinforcement and renovation of existing building inspection projects,” Alexandria Engineering Journal, vol. 82, pp. 240-247, 2023. https://doi.org/10.1016/j.aej.2023.09.075

[4] Y. Tan, W. Xu, P. Chen, and S. Zhang, “Building defect inspection and data management using computer vision, augmented reality, and BIM technology,” Automation in Construction, vol. 160, 2024. https://doi.org/10.1016/j.autcon.2024.105318

[5] E. Szafranko, and M. Jurczak, “Implementability of BIM Technology in Light of Literature Studies and Analyses of the Construction Market,” Sustainability, vol. 16, no. 3, 2024. https://doi.org/10.3390/su16031083

[6] W. Sun, and L. Zhao, “BIM-Based Building Performance Simulation Analysis: A Multi-Parameter-Driven Approach to Building Energy Efficiency and Carbon Reduction,” International Journal of Pattern Recognition and Artificial Intelligence, vol. 37, no. 15, 2023. https://doi.org/10.1142/S0218001423540198

[7]] D. Su, M. Fan, and A. Sharma, "Construction of Lean Control System of Prefabricated Mechanical Building Cost Based on Hall Multi-dimensional Structure Model," Informatica-an International Journal of Computing and Informatics, vol. 46, no. 3, pp. 421-428, 2022. https://doi.org/10.31449/inf.v46i3.3914

[8] X. Shi, and L. Wang, “Distribution Technique of Green Material List for High-Rise Building Engineering in BIM Technology,” Mathematical Problems in Engineering, vol. 2022, 2022. https://doi.org/10.1155/2022/6960596

[9] Y. X. Shen, and Y. Pan, “BIM-supported automatic energy performance analysis for green building design using explainable machine learning and multi-objective optimization,” Applied Energy, vol. 333, 2023. https://doi.org/10.1016/j.apenergy.2022.120575

[10] C. Shen, B. Jiang, and L. Yue, “LSTM combined with BIM technology in the management of small and medium-sized span highway concrete beam bridges,” Results in Engineering, vol. 20, 2023. https://doi.org/10.1016/j.rineng.2023.101539

[11] J. Shao, W. Yao, P. Wang, Z. He, and L. Luo, “Urban GeoBIM Construction by Integrating Semantic LiDAR Point Clouds With as-Designed BIM Models,” Ieee Transactions on Geoscience and Remote Sensing, vol. 62, 2024. 10.1109/TGRS.2024.3358370

[12] B. Melnikov, and A. Melnikova, "A new algorithm of constructing the basis finite automaton," Informatica, vol. 13, no. 3, pp. 299-310, 2002. https://doi.org/10.3233/INF-2002-13304

[13] S. M. E. Sepasgozar, A. A. Khan, K. Smith, J. G. Romero, X. Shen, S. Shirowzhan, H. Li, and F. Tahmasebinia, “BIM and Digital Twin for Developing Convergence Technologies as Future of

Digital Construction," Buildings, vol. 13, no. 2, 2023. https://doi.org/10.3390/buildings13020441
[14] E. van 't Wout, "Stable and efficient FEM-BEM coupling with OSRC regularisation for acoustic wave transmission," Journal of Computational Physics, vol. 450, 2022. https://doi.org/10.1016/j.jcp.2021.110867
[15] A. Talebi, F. Potenza, and V. Gattulli, "Interoperability between BIM and FEM for vibration-based model updating of a pedestrian bridge," Structures, vol. 53, pp. 1092-1107, 2023. https://doi.org/10.1016/j.istruc.2023.04.115
[16] D. Stocco, M. Larcher, M. Tomasi, and E. Bertolazzi, "TRUSSME-FEM: A toolbox for symbolic-numerical analysis and solution of structures," Computer Physics Communications, vol. 309, 2025. https://doi.org/10.1016/j.cpc.2024.109476
[17] H. Fan, B. Goyal, and K. Z. Ghafoor, "Computer-Aided Architectural Design Optimization Based on BIM Technology," Informatica-an International Journal of Computing and Informatics, vol. 46, no. 3, pp. 323-332, 2022. https://doi.org/10.31449/inf.v46i3.3935
[18] G. Silva, A. Quispe, J. Baldoceda, S. Kim, G. Ruiz, M. A. Pando, J. Nakamatsu, and R. Aguilar, "Additive construction of concrete deep beams using low-cost characterization methods and FEM-based topological optimization," Construction and Building Materials, vol. 418, 2024. https://doi.org/10.1016/j.conbuildmat.2024.135418
[19] B. Shi, X. Wang, Q. Dong, X. Chen, X. Gu, B. Yang, S. Yan, and S. Wang, "Voids prediction beneath cement concrete slabs using a FEM-ANN method," International Journal of Pavement Engineering, vol. 24, no. 1, 2023. https://doi.org/10.1080/10298436.2023.2191198
[20] H. Yu, S. Guo, W. Liu, and R. Gao, "Experimental study on stable bearing capacity of wheel-buckle formwork support frames," Structures, vol. 48, pp. 1175-1189, 2023. https://doi.org/10.1016/j.istruc.2023.01.010
[21] L. NamGi, "Development and Implementation of a Low-noise and Safe Dismantling Method for Full-Span Aluminum Slab Formwork Supported by Filler Supports," Journal of the Korea Institute of Building Construction, vol. 24, no. 2, pp. 261-271, 2024. https://doi.org/10.5345/JKIBC.2024.24.2.261
[22] P. T. Mirzaev, and L. P. Shamansurova, "Reinforced Concrete Posts Made by Long-Line Formwork-Free Shaping for 0.4-10 kV Overhead Line Supports," Science & Technique, vol. 21, no. 4, pp. 314-322, 2022. https://doi.org/10.21122/2227-1031-2022-21-4-314-322
[23] Z. Lu, and C. Guo, "Probabilistic analysis of derrick frame in a formwork support system," Ain Shams Engineering Journal, vol. 14, no. 5, 2023. https://doi.org/10.1016/j.asej.2022.101977
[24] M. Lopez Rey, and R. Chercoles Asensio, "Material study by FTIR-ATR and morphological examination for the use of formwork pipes as storage support for tapestries," Ge-Conservacion, no. 21, pp. 7-15, 2022. https://hdl.handle.net/20.500.14352/93671
[25] A. Karasan, E. K. Zavadskas, C. Kahraman, and M. Keshavarz-Ghorabaee, "Residential Construction Site Selection Through Interval-Valued Hesitant Fuzzy CODAS Method," Informatica, vol. 30, no. 4, pp. 689-710, 2019. https://doi.org/10.3233/INF-2019-1232
[26] W. Liu, L. He, J. Liu, X. Xie, N. Hao, C. Shen, and J. Zhou, "Design Optimization of an Innovative Instrumental Single-Sided Formwork Supporting System for Retaining Walls Using Physics-Constrained Generative Adversarial Network," Buildings, vol. 15, no. 1, 2025. https://doi.org/10.3390/buildings15010132
[27] A. Kandiri, P. Shakor, R. Kurda, and A. F. Deifalla, "Modified Artificial Neural Networks and Support Vector Regression to Predict Lateral Pressure Exerted by Fresh Concrete on Formwork," International Journal of Concrete Structures and Materials, vol. 16, no. 6, pp. 917-938, 2022. https://doi.org/10.1186/s40069-022-00554-4
[28] M. Ji, F. Zeng, Y. Dong, and Y. Fan, "Calculation Method of Stable Bearing Capacity of Fastener-Type Steel Pipe Formwork Support Upright Rod," Applied Sciences-Basel, vol. 13, no. 8, 2023. https://doi.org/10.3390/app13084838
[29] X. Cao, X. Wang, Z. Zhang, H. Zhao, S. Wang, X. Cao, and M. Liu, "Surrounding rock activity law and support optimization of double flexible formwork wall gob-side entry retention in stratified mining coal seams," Energy Exploration & Exploitation, vol. 41, no. 3, pp. 1141-1168, 2023. https://doi.org/10.1177/01445987221148876
[30] A. Baghi, N. Aminpour, A. Memari, S. Bilen, S. Nazarian, and J. P. Duarte, "3D concrete printing of self-supported filaments via entrained cables: constructing formwork-free spanning structures," Virtual and Physical Prototyping, vol. 19, no. 1, 2024. doi:10.26207/7yzb-je50.
[31] X.-w. Zhou, F.-t. Liu, B.-b. Dai, C.-b. Zhang, and J.-p. Zhang, "Limit analysis method based on mixed constant stress-smoothed strain element," Rock and Soil Mechanics, vol. 43, no. 6, pp. 1660-1670, 2022. 10.20174/j.JUSE.2024.02.27
[32] M. J. Zhao, P. C. Zhu, Z. Li, Z. Liu, and C. Kang, "Stress Analysis of Self-Tightness Metal Sealing Against Ultrahigh Pressure Medium," Strength of Materials, vol. 54, no. 1, pp. 108-116, 2022. https://doi.org/10.1007/s11223-022-00390-7
[33] Z. Zhang, N. Wang, K. Pi, Z. Wu, M. Su, D. Zhu, Z. Xie, Q. Wu, M. Peng, and R. Li, "Stress Analysis of Vibrating Screen Side Plate based on Elastic Theory," Mechanika, vol. 30, no. 5, pp. 449-457, 2024. https://doi.org/10.5755/j02.mech.37285

[34] K. Sutiene, D. Makackas, and H. Pranevicius, "Multistage K-Means Clustering for Scenario Tree Construction," Informatica, vol. 21, no. 1, pp. 123-138, 2010. https://doi.org/10.3233/INF-2010-21(1)09